

# **Electrical Properties of Undoped and Doped MOVPE-grown InAsSb**

T.Krug, L.Botha, P.Shamba, T.R.Baisitse, A.Venter, J.A.A.Engelbrecht and  
J.R.Botha  
Department of Physics, Nelson Mandela Metropolitan University, Port Elizabeth,  
South Africa

## Abstract

Strong surface inversion usually leads to deceptive Hall measurements by reflecting typical n-type behaviour for p-type samples, especially at very low doping concentrations. A two-layer model is presented which can potentially be used to extract the bulk layer properties of a semiconductor epilayer. We here apply this model to two different materials, InAs and InAsSb, and extract their transport properties.

## Introduction

The ternary alloy  $\text{InAs}_{1-x}\text{Sb}_x$  has become an important candidate for long-wavelength optoelectronic devices and optical gas sensor applications due to its possible bandgap range from about 0.1 to 0.36 eV [1, 2]. Furthermore the reported electron mobilities for the undoped materials are very high compared with GaAs [3]. Therefore the material also promises significant potential for high-speed device applications. There is particular interest in the alloy composition corresponding to  $x=0.09$  [4], which is lattice matched to GaSb substrates and which corresponds to a room temperature energy gap of approximately 4.2  $\mu\text{m}$ , appropriate to cover the atmospheric window in the wavelength range of 3-5  $\mu\text{m}$ , where minimum absorption is present.

In this paper we report on the electrical properties of InAs and InAsSb layers grown by atmospheric pressure metalorganic vapour phase epitaxy (MOVPE). The electrical properties of the undoped InAs layers are evaluated by Hall measurements. The bulk and the surface accumulation layer are treated as a two-layer model, which allows the extraction of mobility and carrier concentration values for the bulk of the epilayer.

These values are then compared to results obtained by infrared reflectance spectroscopy. In addition to the properties of undoped layers, the incorporation of Zn as a p-type dopant is investigated using the same methods. As a source for p-doping, the metal organic dimethylzinc (DMZn) was used. Previous reports show that normally diethylzinc (DEZn) is used as a p-dopant due to its lower cracking temperature [5].

## Experimental

In order to perform Hall measurements, the  $\text{InAs}_{1-x}\text{Sb}_x$  ( $x \leq 0.1$ ) layers were grown on semi-insulating GaAs substrates, misorientated by  $2^\circ$  from (100), at atmospheric pressure using arsine, trimethylindium (TMIn) and trimethylantimony (TMSb). The substrate temperature  $T_G$  was varied from 575  $^\circ\text{C}$  to 625  $^\circ\text{C}$ . The V/III ratio has been varied from 2 to 10, at a growth rate of  $\sim 2.5 \mu\text{m/h}$ . Growth of InAsSb, using a V/III ratio of 2.1 gave the best results in terms of Sb incorporation efficiency and manageable arsine flow control (due to a limited mass flow controller range). A molar flow rate of  $6.5 \times 10^{-6}$  mol/min was used for TMIn. P-type doping was achieved by using DMZn (200 ppm in  $\text{H}_2$ ).

The GaAs substrates were not subject to any pre-growth cleaning steps and were just dusted with N<sub>2</sub> after cleaving.

The concentration of Sb was obtained by x-ray diffraction using the 400 reflection. The uncertainty in the measured Sb content is  $\Delta x = 0.02$ . The thickness of the InAsSb layer was found by etching a cleaved sample in Murakami-etch for about 10 sec. The etch line between the substrate and the InAsSb layer could then be resolved using a Nomarski differential interference contrast microscope. Measurements for undoped InAsSb layers gave a thickness of  $\sim 7 \mu\text{m}$ .

The magnetic field response of the resistance and the Hall coefficient of the InAsSb layers were studied over a wide range of temperatures and magnetic field strengths using the Van der Pauw technique. The ohmic contacts were made of indium and were annealed under N<sub>2</sub> flow for 5min at 350 °C. The samples were mounted on the cold finger of a closed cycle helium refrigerator, which was positioned in an electromagnet of maximum field strength of  $\leq 0.5 \text{ T}$ . The data reading and temperature control of the cryostat was processed by a computer.

The electron concentration and mobility of an InAs epilayer at room temperature has also been studied using infrared reflectance spectroscopy. The undoped InAs layer (M3007) was grown on 2° off (100) InAs substrate, with a substrate temperature of 650 °C and a V/III ratio of 5. The thickness of the epilayer was measured to be 3  $\mu\text{m}$  by Nomarski differential interference method. The infrared reflectivity spectrum of the layer was measured at 8cm<sup>-1</sup> resolution in the frequency range 200-1400 cm<sup>-1</sup> on a Nicolet Magma 550 Fourier Transform Infrared (FTIR) Spectrophotometer.

### Results and Discussion

Optical investigation of the surface morphology using a light microscope showed an improvement in surface morphology with increasing growth temperature. However, for temperatures above 600 °C the Sb incorporation in the sample dropped [4]. At 575 °C a greater amount of Sb was incorporated in the sample and the surface was found to be still relatively smooth.

## InAs

In order to establish and present two ways of measuring the electrical properties of the grown epilayers, the models for the two layer Hall effect analysis and the infrared reflectance spectroscopy were first applied to two InAs layers grown on GaAs. The thicknesses of these layers are 16  $\mu\text{m}$  and 22  $\mu\text{m}$ , respectively. Both layers were grown at  $T_G = 650$  °C with a V/III ratio of 10. Transport measurements of InAs are known to be affected by strong surface accumulation effects due to a line-up of the surface Fermi energy above the conduction band [6]. For relatively thin, high purity layers, the accumulation layer results in sheet concentrations that can be considerably higher than the concentration of the bulk layer alone [7]. The presence of the accumulation layer results in a reduction in the observed electron mobility determined by conventional Hall measurements compared with the bulk value due to scattering at the surface.

In order to quantify the carrier concentration and mobility for the surface layer and bulk layer of the material independently a two layer model has been applied. The following expressions are defined by the two-layer model of Nedoluha and Koch [8].

$$\sigma_0 = \frac{\mu_b n_b e d_b + \mu_s n_s e d_s}{d} \quad (1)$$

$$R_H = d \left[ \frac{\mu_b \mu_b n_b e d_b + \mu_s \mu_s n_s e d_s + \mu_b \mu_s (\mu_b n_b e d_b + \mu_b \mu_s n_s e d_s) B^2}{(\mu_b n_b e d_b + \mu_s n_s e d_s)^2 + (\mu_s \mu_b n_b e d_b + \mu_b \mu_s n_s e d_s)^2 B^2} \right] \quad (2)$$

$$\frac{\Delta\rho}{\rho_0} = \frac{(\mu_b - \mu_s)^2 \mu_b n_b d_b \mu_s n_s d_s (eB)^2}{(\mu_b n_b e d_b + \mu_s n_s e d_s)^2 + (\mu_s \mu_b n_b e d_b + \mu_b \mu_s n_s e d_s)^2 B^2} \quad (3)$$

Equation (1) states the zero-B-field conductivity of the sample. Equation (2) gives the Hall coefficient as a function of the magnetic field B for an n-type surface layer on an n-type epilayer and Equation (3) is an expression of the magnetoresistivity as a function of the magnetic field. Here, e is the elementary charge and d is the measured layer thickness,  $\mu_{b,s}$ ,  $n_{b,s}$  and  $d_{b,s}$  are the mobility, carrier concentration and thickness and the subscripts b and s denote the bulk and surface layer, respectively. The surface layer thickness can be approximated by the Debye length. For a specific temperature

all three quantities,  $\sigma_0$ ,  $R_H$  vs.  $B$  and  $\rho$  vs.  $B$  can be measured. To overcome the problem of having more unknown variables than equations and therefore dealing with an under determined system, the following new approach has been applied. First the following set of variables is defined:

$$\alpha = (\mu_b n_b e d_b + \mu_s n_s e d_s)^2 \quad (4)$$

$$\beta = \mu_b \mu_b n_b e d_b + \mu_s \mu_s n_s e d_s \quad (5)$$

$$\theta = \mu_s \mu_b n_b e d_b + \mu_b \mu_s n_s e d_s \quad (6)$$

$$\gamma = (\mu_b - \mu_s)^2 \mu_b n_b e d_b \mu_s n_s e d_s \quad (7)$$

$$\kappa = \mu_b \mu_s \quad (8)$$

Substituting Equations (4)-(8) into Equation (1)-(3) gives the following expressions:

$$\sigma_0 = \frac{\sqrt{\alpha}}{d} \quad (9)$$

$$R_H = \frac{d[\beta + \kappa \theta B^2]}{[\alpha + \theta^2 B^2]} \quad (10)$$

$$\frac{\Delta \rho}{\rho_0} = \frac{\gamma B^2}{[\alpha + \theta^2 B^2]} \quad (11)$$

By inverting Equation (11), a straight line relationship is obtained:

$$\frac{\rho_0}{\Delta \rho} = \frac{\alpha}{\gamma} B^{-2} + \frac{\theta^2}{\gamma} \quad (12)$$

From Equation (9), the parameter  $\alpha$  can be expressed in terms of measurable quantities. By plotting  $\rho/\rho_0$  vs.  $B^{-2}$ , the slope and the y-intercept of Eq. (12) can be obtained. Equation (10) was employed to obtain  $\beta$  and  $\kappa$ . Once  $\alpha$ ,  $\beta$ ,  $\gamma$ ,  $\theta$  and  $\kappa$  are obtained, the problem can be restated as five equations and four unknown variables. Thus,  $\mu_{b,s}$  and  $n_{b,s}$  can be obtained by solving any four of the five equations simultaneously. In this analysis, Equations (4), (5), (6) and (8) are used. The analytic process of determining  $\alpha$ ,  $\beta$ ,  $\gamma$ ,  $\theta$  and  $\kappa$  however, limits the accuracy of the results. This implies that the possibility to choose different combinations of 4 of these 5 parameters to calculate  $\mu_{b,s}$  and  $n_{b,s}$  will lead to varying degrees of accuracy of the results. Different combinations of the parameters typically show a maximum deviation of up to 33%, relative to any extracted value.

The resulting carrier density and mobility for the surface layer and bulk of the material are presented in Table 1, together with data from Ref. [10] for InAs grown by molecular beam epitaxy. The results of the two-layer model show that the carrier concentration of the bulk of the epilayer is substantially lower than the carrier concentration of the surface accumulation layer. Also, the mobility of the bulk layer is higher than that of the surface layer, and the presence of the surface layer lowers the values for mobility when the conventional Hall equations are used. The peak mobilities for the bulk of the material at 80 K is  $\sim 100,000 \text{ cm}^2/\text{Vs}$ , indicating that the material quality is comparable to what has been previously achieved by MOVPE [7]. The electrical properties of the surface accumulation layer do not show any dependence on temperature [9].

Figure 1 shows the measured reflectivity spectrum of layer M3007 (InAs/InAs) and a best fit simulation spectrum obtained using a derivative free, non-linear regression curve fitting computer program.

Fitting these measured results with an oscillator formula allows for the dielectric properties of the InAs epilayer and the substrate to be assessed simultaneously [11]. Including the layer thickness, a total of 13 variables for both the epilayer and its substrate are obtained. Solving the complex dielectric function for layer and substrate, it was possible to extrapolate the data towards lower wavenumbers and determine the carrier concentration and mobility for layer and substrate from the plasma resonance frequency and free carrier damping constant. The results from the computer curve fitting are presented in Table 2, along with the results from conventional Hall measurements performed on an InAs substrate. The extracted carrier concentration and mobility of the layer are in reasonable agreement with the values of  $n_b$  and  $\mu_b$ , extracted from the two-layer model for the layers discussed above (grown under similar conditions). The values from the simulation for the InAs substrate also show reasonable agreement with the Hall results. It is known that electrical and optical techniques sometimes do not yield exactly the same values [12].

## *InAsSb*

The presented two layer model has been adopted for the treatment of the InAsSb layers. Two series of layers are considered: the substrate temperature during growth was 575 °C for series 1 and 625 °C for series 2 while the corresponding V/III ratios were 2.5 and 10, respectively. Hall data were obtained for both series of layers. By measuring the resistivity, the Hall voltage and the Hall coefficient the carrier concentration and the mobility of the semiconductor material were obtained. The average carrier density and mobility derived from the data is shown in Fig. 2.

Hole concentration of up to  $p = 1 \times 10^{19} \text{ cm}^{-3}$  were measured in Zn doped layers. As with unintentionally doped alloys, the hole-mobility was low for the Zn doped layers and ranged between 105 and 7  $\text{cm}^2/\text{Vs}$ . These results compare very favourable with mobilities measured for similar hole concentrations for MOVPE grown GaInAsSb:Zn [13] and InSb:Zn [14].

The average carrier density for low Zn concentration is n-type and almost constant at  $1 \times 10^{17} \text{ cm}^{-3}$ . For increased Zn flow during the growth process the resulting InAsSb layer becomes p-type and the carrier concentration increases. An average carrier concentration of up to  $p = 1 \times 10^{19} \text{ cm}^{-3}$  has been measured for a Zn flow of 75 cc/min at a V/III ratio of 2.1. For lower growth temperatures (series 1) a higher average carrier concentration is achieved compared to the layers grown with the same zinc flow from series 2. The reported carrier concentration extracted for the bulk of the undoped InAsSb layer (M3172) is considerably higher than the bulk carrier concentration obtained for the InAs samples; this can possibly be attributed to more defects in the ternary material. The lower mobility  $\mu_b$  for the InAsSb layer compared to the InAs epilayer seems to confirm this assumption. It also has to be mentioned also that even though to the extrapolated mobilities for all three layers under investigation stays the same, the number of defects introduced by zinc doping show show an effect on the mobility value. Here the model clearly does not take any intermediate layers between the surface and the bulk into consideration.

The bulk carrier concentration for sample M3174 does not seem to show a compensation effect of the incorporated zinc on the intrinsic doping level,  $n_b$  for sample M3180 however, shows an indication of compensation.

In the present study the two-layer model is only applied to n-doped layers. The model could be easily adapted to accommodate p-doped layers with an n-doped surface accumulation layer but unfortunately all heavily Zn doped layers that were available for this study do not show any or very weak B field dependence of the Hall coefficient for  $B < 0.5$  T. This is due to the fact that for  $p \gg n$  and low mobilities much larger B-fields are necessary to measure this effect [15].

The results obtained by applying the two-layer model to low doped layers are shown in Table 3. For sample M3172 no zinc flow was present and hall measurements indicate that this layer is unintentionally doped with a free carrier concentration at room temperature in the bulk layer of  $n = 9.7 \times 10^{15} \text{ cm}^{-3}$ . Sample m3174 and m3180 are doped with a Zinc flow of 1.5 cc/min and 7.5 cc/min respectively. For InAsSb layers, the two-layer model shows that the carrier concentration of the bulk of the InAsSb epilayer is lower than the carrier concentration of the surface accumulation layer and also by one order of magnitude lower than the carrier concentration extracted from conventional Hall measurements. The mobility of the bulk layer is higher by one order of magnitude than that of the surface layer, and the presence of the surface layer lowers the values for mobility when the conventional Hall equations are used.



## Conclusion:

The electrical properties of undoped InAs layers are evaluated from Hall measurements by using a new analysis method based on a two-layer model. The results are compared with conventional Hall measurement results and values obtained by infrared reflectance spectroscopy. Electron concentrations at room temperature of  $\sim 10^{15} \text{ cm}^{-3}$  have been achieved and confirmed by measurements of the plasma resonance minima in the infrared reflectance spectra. Using the presented two-layer model, the electrical properties of undoped InAsSb and p-type doped InAsSb are also investigated. The results of the two-layer model show that the carrier concentration of the bulk of the epilayer is substantially lower than the carrier concentration of the surface accumulation layer. While the presented analysis has so far only been successfully applied to n-type doped layers, the availability of a higher magnetic field should prove the model useful also for the characterization of p-type material. The analysis can also be a very useful tool to investigate low p-type doped or almost compensated layers for the use in long-wavelength infrared detector applications.

References:

- [1] X.Y.Gong et al., *Cryst. Res. Technol.*, 30, p 103-612, 1995
- [2] R.M.Biefeld, S.R.Kurtz, A.A.Allerman, *IEEE Journal of Selected Topics in Quantum Electronics*, Vol.: 3, Issue: 3, p. 739-748, 1997
- [3] N.V.Zotova, S.S.Kizhaev, S.S.Molchanov, T.B.Popova, Yu.P.Yakovlev, *Semiconductors*, Vol.34, No.12, p.1402-1405, 2000
- [4] R.M.Biefeld, *Journal of Crystal growth*, 75, p 255, 1986
- [5] H.H.Wieder , *Applied Physics Lett.* 25, p 206, 1974
- [6] M.Noguchi, K.Hirakawa and T.Ikoma, *Phys. Rev. Lett.* 66, p.17, 1991
- [7] S.P.Watkins, C.A.Tran, R.Ares and G.Soerensen, *Appl. Phys. Lett.* 66, p.7, 1997
- [8] A.Nedoluha , K.M.Koch, *Zeitschrift der Physik* 132, p.608, 1952
- [9] J.R.Botha, V.Vankova, L.Botha, P.Gladkov, *Proceedings of the 12<sup>th</sup> International Conference on Narrow Gap Semiconductors*, Institute of Physics Conference Series Vol 187, p113-118, 2006
- [10] P.D.Wang, S.N.Holmes, Le.Tan, R.A.Stradling, I.T.Ferguson and de A.D.Oliveira, *Semicond. Sci. Technol.* 7, p.767 – 786 ,1992
- [11] J.A.A. Engelbrecht, J.R.Botha, *Phys.Stat.Sol.*, 1, No.9, p 2349, 2004
- [12] S.Perkowitz and R.H.Thorland, *Phys.Rev.B* 9,p.545, 1974
- [13]C.A.Wang, H.K.Choi, D.C.Oakley, G.W.Charache, *Journal of Crystal Growth*, 195, p.346-355, 1998
- [14] R.M.Biefeld. S.R.Kurtz, I.J.Fritz, *J.Electron Materials* 18, p.775, 1989
- [15] D.K.Schroder, *Semiconductor material and device characterization*, 2<sup>nd</sup> Edition, Wiley-Interscience, p 513

**Table 1. Comparison of results obtained for two InAs/GaAs layers with those of Wang et al [10].**

d	T (K)	$n_s$ (cm <sup>-3</sup> )	$n_b$ (cm <sup>-3</sup> )	$n$ (cm <sup>-3</sup> )	$\mu_s$ (cm <sup>2</sup> /Vs)	$\mu_b$ (cm <sup>2</sup> /Vs)	$\mu$ (cm <sup>2</sup> /Vs)
16 $\mu$ m	80	$3 \times 10^{18}$	$3 \times 10^{14}$	$1 \times 10^{16}$	$5 \times 10^3$	$1 \times 10^5$	$2 \times 10^4$
22 $\mu$ m	81	$1 \times 10^{18}$	$2 \times 10^{14}$	$3 \times 10^{15}$	$7 \times 10^3$	$1 \times 10^5$	$3 \times 10^4$
17 $\mu$ m <sup>a</sup>	77	$1 \times 10^{17}$	$2 \times 10^{14}$	-	$2 \times 10^4$	$2 \times 10^5$	-

<sup>a</sup> Carrier concentration and mobility given in Wang et al [10] for a 17 $\mu$ m InAs film grown on GaAs by molecular beam epitaxy. These results were obtained using cyclotron resonance measurements.

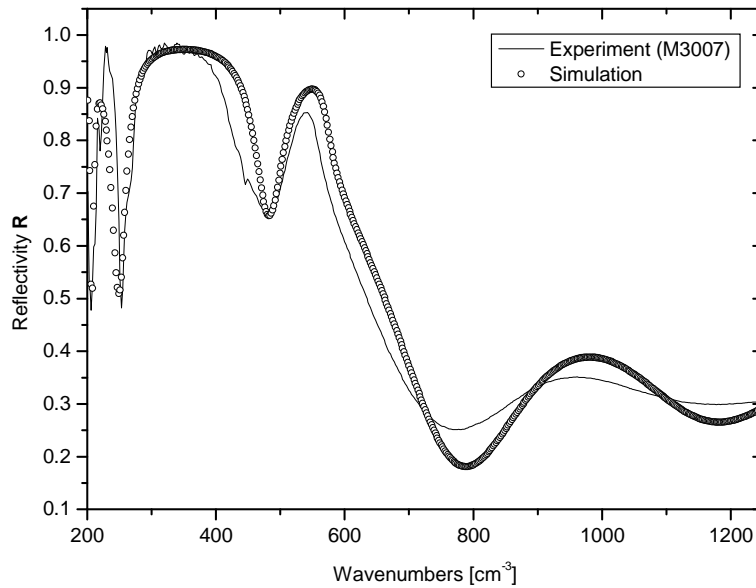


**Figure 1: Reflectance spectrum of M3007, together with computer simulation result.**

**Table 2: Carrier concentration and mobility for layer and substrate (sample M3007) obtained by infrared reflectance characterization (Simulation). Transport parameters obtained by conventional Hall measurements are also shown for comparison (Measured).**

Sample	Simulation		Measured	
	$n(\text{cm}^{-3})$	$\mu(\text{cm}^2 \text{V}^{-1} \text{s}^{-1})$	$n(\text{cm}^{-3})$	$\mu(\text{cm}^2 \text{V}^{-1} \text{s}^{-1})$
Layer	$1 \times 10^{15}$	$6 \times 10^4$	----	----
Substrate	$1 \times 10^{18}$	$3 \times 10^4$	$2 \times 10^{18}$	$1 \times 10^4$

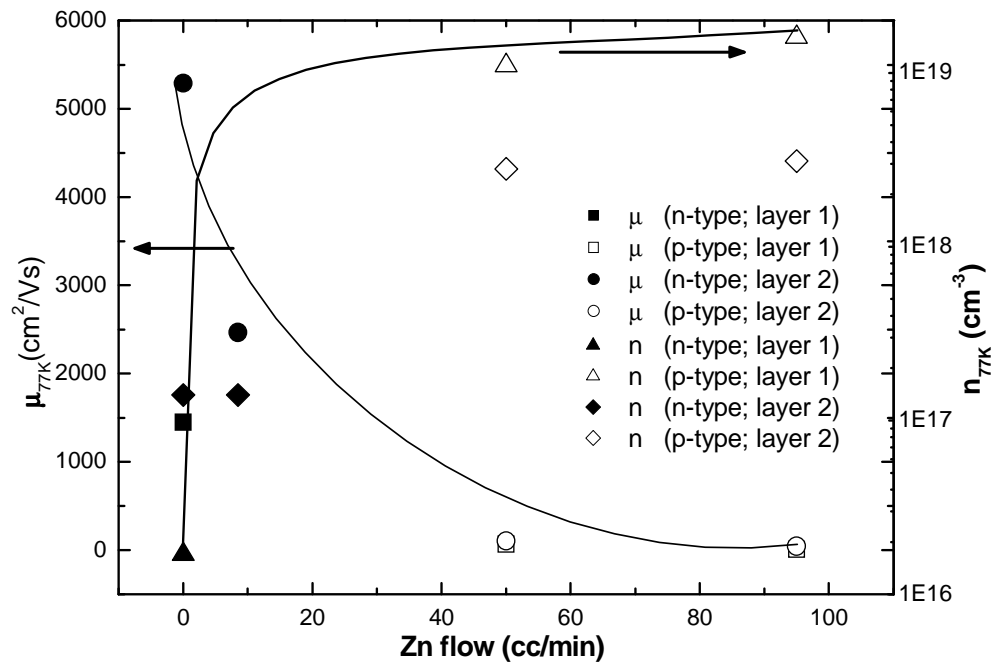


**Figure 2: Electrical properties of two series of  $\text{InAs}_{0.91}\text{Sb}_{0.09}$ , grown at different temperatures and V/III ratios as a function of nominal Zn flow. The two straight lines are a guide to the eye.**

**Table 3: Summary of the parameters extracted for the bulk and surface layer, using the two-layer model.**

Sample	zinc conc. ( $\mu\text{mol}/\text{min}$ )	d( $\mu\text{m}$ )	T(K)	$n_s(\text{cm}^{-3})$	$n_b(\text{cm}^{-3})$	$n(\text{cm}^{-3})$	$\mu_s(\text{cm}^2/\text{Vs})$	$\mu_b(\text{cm}^2/\text{Vs})$	$\mu(\text{cm}^2/\text{Vs})$
M3172	0	7.3	300	$3 \times 10^{19}$	$1 \times 10^{16}$	$7 \times 10^{17}$	$2 \times 10^3$	$2 \times 10^4$	$8 \times 10^3$
M3174	0.013	6.7	92	$7 \times 10^{19}$	$8 \times 10^{15}$	$9 \times 10^{16}$	$2 \times 10^3$	$2 \times 10^4$	$7 \times 10^3$
M3174		6.7	300	$4 \times 10^{19}$	$1 \times 10^{16}$	$1 \times 10^{17}$	$2 \times 10^3$	$2 \times 10^4$	$6 \times 10^3$
M3180	0.063	3.3	300	$6 \times 10^{18}$	$6 \times 10^{14}$	$4 \times 10^{17}$	$2 \times 10^3$	$2 \times 10^4$	$2 \times 10^4$